36th EPS Conference on Plasma Phys. Sofia, June 29 - July 3, 2009 ECA Vol.**33E**, P-1.161 (2009)

Application of AXUV Diodes For Broad-Band Plasma Radiation Studies in ASDEX Upgrade

B. Reiter, G. Pautasso, T. Eich, J. C. Fuchs, L. Giannone, R. Dux. J. Neuhauser, M. Maraschek, V. Igochine, A. Herrmann, T. Lunt and the ASDEX Upgrade Team

Max-Planck-Institut fuer Plasmaphysik, EURATOM Association, D-85748 Garching

Introduction

A multi-channel photometer system was installed and put into operation on ASDEX Upgrade in 2008 for studying fast dynamics of broad-band plasma radiation on the microsecond time scale. Linear arrays of silicon photodiodes - commonly used for *A*bsolute power measurement in the e*X*treme *U*ltra *V*iolet spectral range (*AXUV*) - are encapsulated by pinhole cameras. The plasma is observed by 200 lines of sight, at four different toroidal positions. The AXUV standard detectors have been developed by International Radiation Detectors, Inc [1]. AXUV diodes are characterised by an extremely thin passivation layer, which enables photons of the vacuum-ultraviolet spectral region (VUV) to reach the depletion layer for electron-hole-pair generation. The spectral sensitivity covers the entire energy range from the X-ray down to the visible part of the spectrum. An improvement of the time resolution down to $2\,\mu$s enlarges the insights into radiation dynamics of fast plasma phenomena like minor and major disruptions, sawteeth and edge localised modes, which are not accessible with usual resistive foil bolometers (1 ms time resolution).

In this contribution, a short introduction of the diagnostic is followed by the presentation of first measurements taken during disruption mitigation experiments. The analysis is focussed on the asymmetric evolution of toroidal and poloidal emission after the massive injection of gaseous impurities.

Diagnostic layout

The present setup, shown in Figure 1, is basically designed for measuring the radiative asymmetry during disruption mitigation experiments. The in-vessel gas valve for impurity injection is located on the low-field side at the toroidal angle of $\varphi = 0$ (marked by a blue triangle). At the same φ, two AXUV cameras with 32 lines of sight (*LOS*) view the gas jet from above. Another two identical cameras are mounted at the same poloidal, but opposite toroidal position ($\varphi = \pi$). At $\varphi = \pi$, additional main chamber and divertor AXUV cameras provide a *LOS* coverage of the poloidal cross-section sufficient for tomographic reconstruction. The two camera systems toroidally π away from each other show equal sensitivity as demonstrated in the middle of Figure 1 (same radial radiation profile during an axisymmetric discharge phase). At $\varphi = 0$, there exist also standard resistive metal foil bolometer cameras (24 *LOS*), which can be used for cross-checks of radiation power profiles.

One should notice that even though AXUV diodes are sensitive to photons at all relevant energies, they do not allow for exact bolometric measurements, since the responsivity is reduced by a factor of up to 3 for wavelengths between 100 to 125 nm. Therefore the absolute radiation power recorded by lines of sight with dominant VUV contribution may be wrong by some factor dependent on actual local plasma parameters.

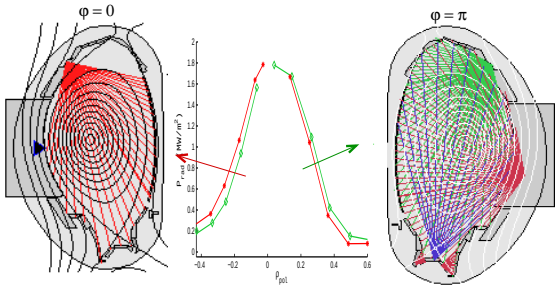

Figure 1: Setup and emission profiles

Radiation Dynamics during Disruption Mitigation Experiments

The results of massive gas injection experiments for disruption mitigation carried out in several tokamaks like Alcator C-Mod [2], JET [3], DIIID [4], TEXTOR [6] or ASDEX Upgrade [7], support this technique for being an effective way of mitigating heat and force loads to the inner wall structure of ITER. For getting a detailed background on disruption mitigation, the reader is referred to the contributions of G. Pautasso et. al. [5] and M. Lehnen et. al. [3] at this conference.

The chronology of a mitigated disruption by massive gas injection (neon puff; ♯ 24442) is shown in Figure 2. The in-vessel gas valve has a capacity of 80 cm^3 and an initial pressure of 4 MPa ($\triangleq$3.2 bar l). The opening trigger of the gas valve is at 2.98 s. The time delay of radiation appearing in front of the valve is of 700 μs. The red solid graph constitutes the mean radiation power ($\langle P_{pol}(\varphi = 0)\rangle$), measured by the AXUV lines of sight at $\varphi = 0$. (AXUV radiation power is calculated assuming a mean responsivity of 0.24 A/W for all cameras - but, arbitrary units are used due to an unknown VUV contribution.) The plasma reacts $\approx$ 200 μs later by a decaying thermal energy, which is represented by the magenta line. Another 100 μs delayed, the radiation toroidally π away from the gas valve rises, shown by the green solid curve ($\langle P_{pol}(\varphi = \pi)\rangle$). It stays rather unaffected by the strong dynamics near the valve on the other side of the torus. This smooth behaviour ends abruptly when the temperature in the plasma core drops. The radiated power increases rapidly, showing extremely short rise times of down to 10 μs in some disruptions. A central *LOS* of the soft X-ray diagnostic (solid, black graph) is used here as an indicator for the loss of core thermal energy. This core signal remains essentially constant during the cooling time t_{cool}, which implies that in this phase only edge energy is radiated, leaving the core essentially unaffected. This is also supported by tomographic radiation profile reconstructions (at $\varphi = \pi$) during this time window, which shows emission only in the edge. Finally, the plot contains also the temporal integrals (dashed red and green lines) of the radiation powers in both poloidal planes ($\varphi = 0$ and π), which gives an indication for the asymmetry of the radiated energy up to the respective time ($E(t) = \int dt \langle P_{pol}(\varphi, \mathrm{t})\rangle$). In this particular case, the two values become nearly equal after about 4 ms.

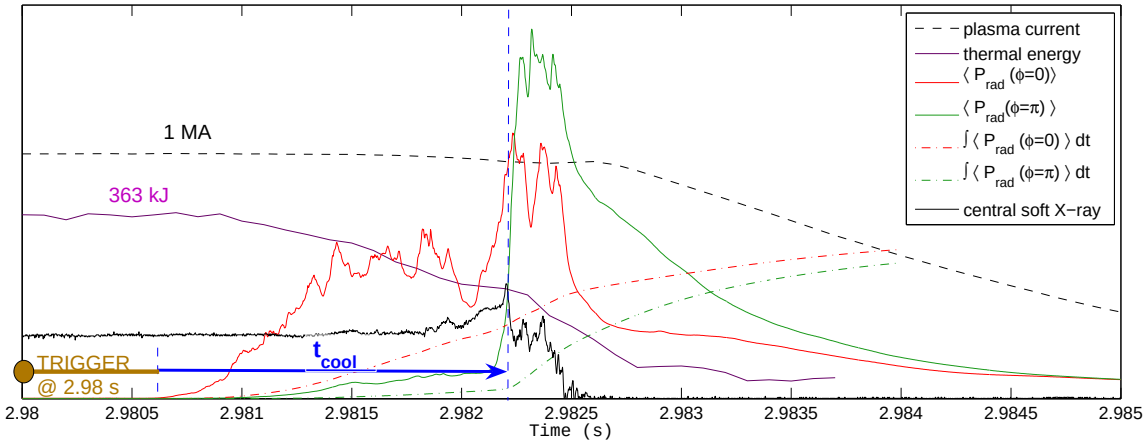

Figure 2: Basic chronology of mitigated disruptions.

The delay between valve trigger and the first radiation in front of the valve (thick orange line), captured by the AXUV lines of sight viewing the valve directly from above, is due to the neutral transit time. It is different for neon and argon and scales basically with the square root of the mass ratio $\sqrt{M_{Ar}/M_{Ne}}$. The maximal delay for argon is of about 1 ms.

The cooling time interval (thick blue arrow) is defined as the duration between the first radiation in front of the valve and the core soft-X ray drop. Looking now in more detail on the AXUV radition signals from both poloidal planes, we find that at $\varphi = 0$ the radiation rises in the beginning rather smoothly, while the diodes toroidally π away do not react yet at all. At this time, a tangentially viewing CMOS camera with a time resolution of 27.8 μs detects the impurity radiation as a small spot, which elongates poloidally and splits up into two separated spots after roughly 130 μs. This onset of filament type perturbations and fragmentation is seen also in two (faster) AXUV lines of sight as a start of frequent fluctuations. Figure 3 shows the corresponding geometry, some of the relevant CMOS frames and the two AXUV signals as function of time. The variable time shift between the blue and red AXUV channels may indicate a slowly changing filament rotation. This is still under investigation.

Approximately 80 μs delayed, the radiation rises also at $\varphi = \pi$, where a tomographic reconstruction shows bright spots at the top of the poloidal cross-section (see Figure 3 on the right), qualitatively consistent with initial impurity plasmoid expansion along magnetic field lines half around the torus.

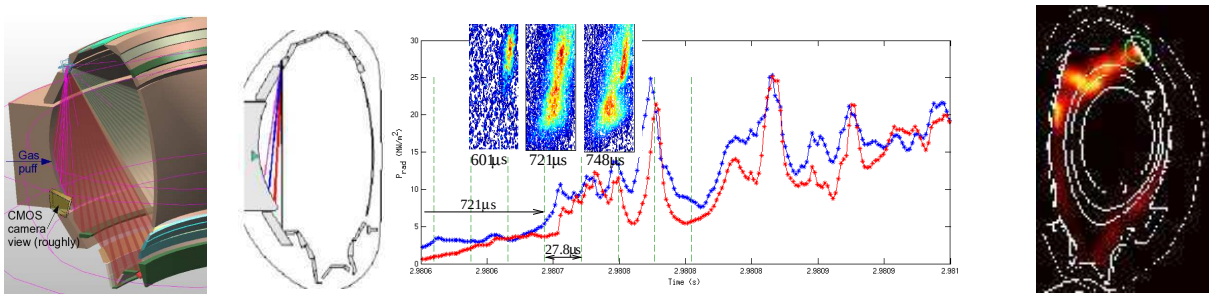

Figure 3: Initial radiation evolution in front of the valve and first arrival at the opposite torus side. The two graphs on the left: geometry of top AXUV channels and tangential CMOS camera view. Middle: filaments on CMOS frames and corresponding fluctuations on two AXUV signals. The time delays relativ to the gas valve trigger, are inserted in the graph. Right: tomographic reconstruction of radiation at the opposite torus cross-section at 1506 μs after the valve trigger (the green circle marks a possible artefact)

The thermal collapse (indicated by the fast drop of the central soft-X ray signal) is characterised - in the case of a neon puff (♯24399, t = 2.98212 s) - by strong radiation in form of a ring surrounding the core plasma. This can be seen on the tomographic reconstruction of the poloidal radiation distribution at $\varphi = \pi$ during this phase as shown by the image in Figure 4. The q=2 surface is marked by the inner most white line, which is almost reached by the cooling front. After the high radiation peaks, the remaining radiation was mainly found in front of the lower part of the inner heat shield. A more detailed analysis of the AXUV data and the disruption dynamics is under way.

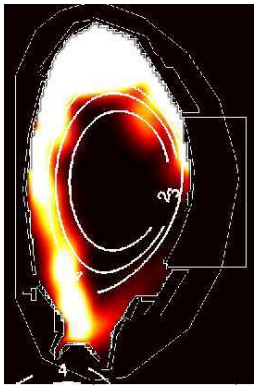

Figure 4: Start of thermal collapse.

Conclusions

A multichannel AXUV photometer system has been installed at ASDEX Upgrade for broad band radiation studies of fast plasma phenomena like sawteeth, edge localised modes and disruptions. First results for the ITER relevant disruption mitigation experiments by massive gas injection were presented. The radiation history was sketched from the first photoresponse in form of a spot in front of the gas valve, followed by its filamentation and expansion into an asymmetric edge radiation around the torus, the thermal collapse and the final decay. Altogether, the results demonstrate the high diagnostic potential of the system.

[1] E.M.Gullikson, et. al., Journal of Electron Spectroscopy and Related Phenomena 80 (1996)
[2] R.Granetz, et. al., Nucl. Fusion; 46 (2006) 1001-1008
[3] M. Lehnen et. al.: First experiments on massive gas injection at JET
[4] D. G. Whyte, et. al., Phys. Rev. Letters; 89(5) (2006)
[5] G. Pautasso et. al.: Disruption studies in view of ITER. Contribution at this conference
[6] S.A.Bozhenkov et. al.,Plasma Phys. Control. Fusion 50 (2008) 105007.
[7] G. Pautasso et. al., Nucl. Fusion 47 (2007) 900-913.